Annals of Nuclear Medicine Vol. 19, No. 4, 251–260, 2005

Effects of tissue heterogeneity on cerebral vascular response to acetazolamide stress measured by an I-123-IMP autoradiographic method with single-photon emission computed tomography

Hiroshi Ito,* Miho Shidahara,* Kentaro Inoue,* Ryoi Goto,* Shigeo Kinomura,* Yasuyuki Taki,* Ken Okada,* Tomohiro Kaneta,** Kazunori Sato,* Tachio Sato* and Hiroshi Fukuda*

*Department of Nuclear Medicine and Radiology, Division of Brain Sciences Institute of Development, Aging and Cancer, Tohoku University
**Department of Radiology, Graduate School of Medicine, Tohoku University

Objectives: Single-photon emission computed tomography (SPECT) with iodine-123 (^{123}I)-labeled *N*-isopropyl-*p*-iodoamphetamine (IMP) is widely used in measuring the cerebral blood flow (CBF) response to acetazolamide stress for assessment of cerebral vascular reserve. To quantitate CBF by means of SPECT with IMP, an autoradiographic (ARG) method has been developed and is widely used. Because the relation between the brain counts on the SPECT scan and CBF is not linear in the ARG method, a mixture of gray and white matter in a pixel causes errors in the calculation of CBF. In the present study, errors in the calculation of CBF and vascular response to acetazolamide stress by the ARG method due to tissue heterogeneity were estimated by simulation study. Correction for effects of tissue heterogeneity in SPECT data was also attempted. ***Methods:*** Images of gray and white matter fraction were obtained by voxel-based morphometry analysis of magnetic resonance (MR) imaging data set. Ideal CBF images, which were generated from gray and white matter fraction images with assumed blood flow values for gray and white matter, were compared to CBF images generated by the ARG method. Correction for effects of tissue heterogeneity in SPECT data was performed with gray and white matter fraction data obtained from MR images. ***Results:*** Systematic underestimation of CBF due to tissue heterogeneity was observed in all brain regions. In the neocortical regions, underestimation by −21% to −16%, −26% to −20%, −31% to −24%, and −35% to −27% was observed for gray and white matter blood flow of 80 and 20, 100 and 25, 120 and 30, and 140 and 35 m*l*/100 m*l*/min, respectively. Vascular response was also systematically underestimated in most brain regions. Vascular responses in the neocortical regions ranged from 17% to 20%, from 31% to 37%, and from 42% to 52% when ideal vascular responses were 25%, 50%, and 75%, respectively. After correction for the effects of tissue heterogeneity, values of vascular response to acetazolamide stress ranged from 64% to 116% in the neocortical regions, whereas values obtained by the ARG method ranged from 48% to 52%. ***Conclusion:*** Underestimation of the vascular response to acetazolamide stress due to tissue heterogeneity should be considered in the estimation of cerebral vascular reserve.

Key words: IMP, SPECT, acetazolamide, ARG method, tissue heterogeneity

INTRODUCTION

Iodine-123 (^{123}I)-labeled *N*-isopropyl-*p*-iodoamphetamine (IMP)[1,2] has been used as a cerebral blood flow (CBF) tracer for single-photon emission computed tomography (SPECT) to investigate the pathophysiology of several brain diseases, particularly occlusive cerebrovascular

Received November 24, 2004, revision accepted February 18, 2005.

For reprint contact: Hiroshi Ito, M.D., Ph.D., Department of Nuclear Medicine and Radiology, Division of Brain Sciences, Institute of Development, Aging and Cancer, Tohoku University, 4–1 Seiryo-machi, Aoba-ku, Sendai 980–8575, JAPAN.
E-mail: hito@idac.tohoku.ac.jp

disease.[3,4] Decreased cerebral perfusion pressure due to major cerebral arterial occlusive disease causes cerebral autoregulatory vasodilatation to maintain CBF.[5] To assess such hemodynamic compromise, the CBF response to acetazolamide, which is a cerebral vasodilator, is measured by SPECT as an indicator of cerebral vascular reserve. Reduced vasodilatory capacity as determined by the acetazolamide stress test is a major predictor of stroke recurrence.[6,7]

To quantitate CBF by IMP-SPECT, an autoradiographic (ARG) method has been developed[8–10] and is used widely to measure the CBF response to acetazolamide stress.[11] With the ARG method, CBF is calculated from the brain counts on the SPECT image with an assumed distribution volume of IMP (V_d) according to the standard single-tissue compartment model. The limited spatial resolution of the SPECT scanner results in representation of both gray and white matter in a single pixel. Because the relation between the brain counts and CBF is not linear in the ARG method,[8] this tissue heterogeneity causes errors in the calculation of CBF by the ARG method.[9,12,13] In particular, errors in CBF values due to tissue heterogeneity are greater when CBF is increased, i.e., during acetazolamide stress.[12] However, regional differences in these CBF calculation errors have not been investigated in detail.

Images of specific brain tissue components, i.e., gray matter, white matter, and cerebrospinal fluid, can be segmented and extracted from magnetic resonance (MR) images with the use of a recently developed voxel-based morphometry (VBM) technique.[14] In the present study, regional differences in errors in CBF values determined by the ARG method due to tissue heterogeneity were investigated with the use of images of gray and white matter fraction derived from MR images by VBM analysis. Regional differences in errors in the vascular response to acetazolamide stress were then estimated. We also attempted to correct effects of tissue heterogeneity in SPECT data using gray and white matter fraction data obtained from MR images.

MATERIALS AND METHODS

Subjects

SPECT studies were performed on eight patients (seven men and one woman, mean age ± SD: 67 ± 16 years, age range: 34–82 years) with a unilateral steno-occlusive lesion of a major cerebral artery. All patients underwent MR imaging and angiography or MR angiography of the brain. All patients were chronically ill.

A total of 28 healthy subjects (16 men and 12 women, mean age ± SD: 61 ± 5 years, age range: 55–71 years) were recruited and gave written informed consent to participate in MR imaging studies with VBM analysis. The subjects were judged healthy on the basis of their medical history, a physical examination, and MR imaging of the brain. The study was approved by the Ethics Committee of the Institute of Development, Aging and Cancer, Tohoku University.

SPECT study in patients

Two SPECT studies were performed on separate days. The first study (baseline) was performed at rest and the second during acetazolamide stress. The interval between the two studies was 2–7 days. For both studies, SPECT scanning was performed at a mid-scan time of 40 min after intravenous infusion of 111 MBq IMP for 1 min. For the acetazolamide stress study, acetazolamide (1 g) was administered intravenously for 1 min starting 10 min before the beginning of IMP infusion. One-point arterial blood sampling from the brachial artery was performed at 10 min after the start of IMP infusion to measure both the radioactivity concentration of whole blood and arterial blood gases. A SPECT scanner (SPECT-2000H, Hitachi Medico Corp., Tokyo, Japan),[15] with a four-head rotating gamma camera fitted with low-energy, medium-resolution collimators and in-plane and axial resolutions of 10-mm full width at half maximum (FWHM), was used for all measurements. The SPECT scan protocol acquired 64 projections at 25 sec (25 sec × four-head camera = 100 sec total) per projection with 360° continuous rotation of the camera. Images were reconstructed by filtered backprojection with a Butterworth filter, and attenuation correction was done numerically by assuming the object to be elliptical for each slice and the attenuation coefficient to be uniform (0.08 cm^{-1}).[16,17] Correction for scattered photons was not performed. Image slices were set up parallel to the orbito-meatal line and were obtained through the whole brain. A cross-calibration scan was performed with the use of a cylindrical uniform phantom (inner diameter, 16 cm) for calibrating sensitivity between the SPECT scanner and the well-counter system.

MRI study in healthy subjects for VBM analysis

All MRI studies for VBM analysis were performed with a 0.5-Tesla MRI scanner (GE, Milwaukee, WI). Three-dimensional volumetric acquisition of a T1-weighted gradient echo sequence produced a gapless series of thin transverse sections using a SPGR sequence (TE: 7 msec, TR: 40 msec, flip angle: 30°, field of view: 25 cm, acquisition matrix: 256 × 256, slice thickness: 1.5 mm).

Data analysis

All SPECT and MR images were transformed into the standard brain size and shape by linear and nonlinear parameters with the statistical parametric mapping (SPM2) system for anatomic standardization.[18] The PET image and T1-weighted image in the SPM2 system were used as templates of the standard brain for SPECT and MR images, respectively. Thus, the brain images of all subjects had the same anatomic format. Gray matter, white matter, and cerebrospinal fluid images were segmented

and extracted from all anatomically standardized MR images by VBM methods in the SPM2 system.[14] These segmented MR images provide data on the tissue fractions of gray and white matter and fraction of cerebrospinal fluid per pixel (m*l*/m*l*). All anatomically standardized SPECT, gray matter, and white matter images were smoothed with an isotropic Gaussian kernel at a 10-mm FWHM which was the same as the FWHM of the SPECT scanner. Average images of gray and white matter fraction were calculated.

Regions-of-interest (ROIs) were drawn on all anatomically standardized SPECT, gray matter, and white matter images, by referring to the T1-weighted MR image (Fig. 1). Circular ROIs were defined for the pons, midbrain, thalamus, putamen, parahippocampal gyrus, and anterior and posterior parts of cingulate gyrus (16 mm in diameter). Elliptical ROIs were defined for the cerebellar cortex, centrum semiovale, base and convexity side of the frontal cortex, the temporal cortex, cuneus and lateral side of the occipital cortex, and inferior and superior sides of the parietal cortex (16 mm × 32 mm).

From SPECT data, CBF values were calculated for each ROI by the ARG method. With the ARG method, CBF is calculated from the brain counts with V_d assumed to be 40 m*l*/m*l*.[19,20] The arterial input function is determined by calibration of the standard input function with one-point arterial blood sampling at 10 min after IMP infusion. The vascular response to acetazolamide stress was calculated as the percentage of change in CBF:

$$\%\ \text{vascular response} = 100 \cdot (CBF_{ACZ}/CBF_{baseline} - 1) \qquad \text{Eq. 1}$$

where $CBF_{baseline}$ is CBF in the baseline study, and CBF_{ACZ} is CBF during acetazolamide stress.

Simulation study

A simulation study was performed to estimate errors in CBF obtained by the ARG method when the fractions of gray and white matter in a given ROI were changed. The time-activity curves in heterogeneous tissue (0 to 40 min) were generated as mixtures of gray and white matter according to the standard single-tissue compartment model.[21] Blood flow values of the gray and white matter were assumed to be 60–140 m*l*/100 m*l*/min in 5 steps and 15–35 m*l*/100 m*l*/min in 5 steps, respectively.[22,23] The V_d values for gray and white matter were assumed to be the same, 40 m*l*/m*l*.[19,20] The difference between ideal CBF, calculated as gray matter blood flow × gray matter fraction + white matter blood flow × white matter fraction, and CBF calculated by the ARG method (ARG-CBF) on the basis of the generated heterogeneous tissue radioactivity was estimated where the fraction of gray matter varied from 0 to 0.9 m*l*/m*l*, assuming the fraction of cerebrospinal fluid to be 0.1 m*l*/m*l*. The standard input function used in the ARG method was employed to generate tissue time-activity curves.[21] The vascular responses in ideal CBF and ARG-CBF were then calculated with Eq. 1, assuming a baseline ideal CBF to be calculated with 80 and 20 m*l*/100 m*l*/min of gray and white matter blood flow, respectively. Calculated vascular responses in ARG-CBF were compared to those in ideal CBF. In the present simulation, vascular responses in blood flow were assumed to be identical between the gray and white matter, on the basis of previous reports.[24,25]

Regional differences in effects of tissue heterogeneity on CBF images processed by the ARG method were also estimated from average images of the tissue fraction of gray and white matter, which were obtained by VBM analysis. The radioactivities in gray and white matter at 40 min were calculated according to the standard single-tissue compartment model with assumed gray and white matter blood flow values of 60–140 m*l*/100 m*l*/min in 5 steps and 15–35 m*l*/100 m*l*/min in 5 steps, respectively, as mentioned above. Brain radioactivity were mapped by calculation of gray matter radioactivity × gray matter fraction + white matter radioactivity × white matter fraction; gray and white matter fractions were obtained from tissue fraction images of gray and white matter. CBF images were then generated by the ARG method from these maps of brain radioactivity. The difference between ideal CBF images, generated by the equation of gray matter blood flow × gray matter fraction + white matter blood flow × white matter fraction, and ARG-CBF images generated by the ARG method was estimated. Images of the vascular response for ARG-CBF were also generated from ARG-CBF images, assuming a baseline ARG-CBF image to be generated with 80 and 20 m*l*/100 m*l*/min of gray and white matter blood flow, respectively.

Correction for effects of tissue heterogeneity in SPECT data

Brain radioactivity concentration in a ROI (C_{ROI}) can be expressed as follows:

$$C_{ROI} = C_{gray} \cdot TF_{gray} + C_{white} \cdot TF_{white} \qquad \text{Eq. 2}$$

where C_{gray} and C_{white} are the radioactivity concentrations of gray and white matter, respectively, and TF_{gray} and TF_{white} are the tissue fractions of gray and white matter (m*l*/m*l*), respectively. If C_{white} is given, C_{gray} can be calculated for given TF_{gray} and TF_{white}. In the present study, C_{white} was assumed to be the radioactivity concentration in the centrum semiovale, and TF_{gray} and TF_{white} were derived from averaged gray and white matter images. Blood flow values of gray and white matter, f_{gray} and f_{white} (m*l*/100 m*l*/min), were then calculated by the ARG method with the use of C_{gray} and C_{white}, respectively. The ideal CBF value in a ROI, that is, the values corrected for effects of tissue heterogeneity, was calculated as follows[23]:

$$\text{Ideal CBF} = f_{gray} \cdot TF_{gray} + f_{white} \cdot TF_{white} \qquad \text{Eq. 3}$$

The vascular response values were obtained from ideal

Table 1 P_aCO_2, P_aO_2, and pH in SPECT studies

Study	P_aCO_2 (mm Hg)	P_aO_2 (mm Hg)	pH
Baseline	40.2 ± 1.9	85.7 ± 8.8	7.423 ± 0.024
Acetazolamide stress	39.7 ± 3.0	92.3 ± 6.2	7.416 ± 0.018

Values are shown as mean ± SD.

Table 2 CBF at baseline and during acetazolamide stress, and vascular responses to acetazolamide stress on the normal side

Region	CBF (m*l*/100 m*l*/min)		Vascular response (%)
	Baseline	ACZ*	
Cerebellum	37.0 ± 7.5	53.3 ± 11.3	44.5 ± 22.4
Pons	27.1 ± 5.7	39.1 ± 9.0	44.2 ± 20.7
Midbrain	26.5 ± 4.4	37.9 ± 7.6	42.0 ± 10.2
Thalamus	27.8 ± 4.8	39.6 ± 9.4	40.6 ± 15.4
Putamen	31.6 ± 5.8	48.2 ± 10.2	51.8 ± 18.6
Parahippocampal gyrus	26.0 ± 4.7	38.5 ± 7.3	48.6 ± 18.0
Anterior cingulate	27.6 ± 4.3	40.8 ± 8.1	47.4 ± 18.4
Posterior cingulate	28.8 ± 4.7	42.7 ± 7.8	49.0 ± 23.2
Frontal cortex base	28.2 ± 5.3	42.9 ± 9.1	51.5 ± 17.9
Frontal cortex convexity	28.0 ± 5.2	42.0 ± 8.0	50.2 ± 16.9
Temporal cortex	31.6 ± 6.2	47.5 ± 10.6	49.6 ± 17.8
Occipital cortex cuneus	35.4 ± 5.1	52.9 ± 11.0	47.9 ± 18.5
Lateral occipital cortex	29.2 ± 4.5	43.8 ± 9.5	48.8 ± 17.2
Inferior parietal cortex	30.2 ± 5.3	45.1 ± 9.9	48.8 ± 22.2
Superior parietal cortex	28.0 ± 4.4	42.3 ± 8.2	50.1 ± 16.1
Centrum semiovale	18.1 ± 3.0	26.0 ± 4.2	44.4 ± 13.6

Values are shown as mean ± SD.
*ACZ: acetazolamide stress

CBF values calculated by this equation with patient data obtained for the normal side, that is, the side of contralateral to the steno-occlusive lesion in the supratentorial region and ipsilateral to the lesion in the cerebellum, and for the pons and midbrain.

RESULTS

P_aCO_2, P_aO_2, and pH values in each SPECT study are shown in Table 1; no significant differences were observed between the studies. Baseline CBF values and CBF during acetazolamide stress, and vascular responses to acetazolamide stress on the normal side are given in Table 2. Values in the pons and midbrain are also given. In the neocortical regions, CBF values ranged from 28 to 35 m*l*/100 m*l*/min for baseline and from 42 to 53 m*l*/100 m*l*/min during acetazolamide stress. The vascular responses to acetazolamide stress in the neocortical regions ranged from 48% to 52%.

Anatomically standardized T1-weighted MR images and gray and white matter images averaged for all subjects are shown in Figure 2. Tissue fraction values of gray and white matter for each ROI on average images of gray and white matter are given in Table 3. Among the neocortical regions, the tissue fraction of gray matter in an ROI ranged from 0.346 to 0.591 m*l*/m*l*, and the tissue fraction of white matter ranged from 0.275 to 0.549 m*l*/m*l*.

Table 3 Tissue fraction of gray and white matter per given ROI on average images of gray and white matter

Region	Tissue fraction (m*l*/m*l*)	
	Gray matter	White matter
Cerebellum	0.655	0.281
Pons	0.329	0.600
Midbrain	0.380	0.511
Thalamus	0.441	0.475
Putamen	0.539	0.452
Parahippocampal gyrus	0.747	0.146
Anterior cingulate	0.482	0.404
Posterior cingulate	0.495	0.429
Frontal cortex base	0.423	0.423
Frontal cortex convexity	0.451	0.382
Temporal cortex	0.591	0.275
Occipital cortex cuneus	0.473	0.417
Lateral occipital cortex	0.346	0.549
Inferior parietal cortex	0.466	0.420
Superior parietal cortex	0.429	0.328
Centrum semiovale	0.053	0.935

The simulated effects of gray-white matter mixing on CBF values calculated by the ARG method are shown in Figure 3. CBF was systematically underestimated because of tissue heterogeneity. Maximum degrees of underestimation were −15%, −17%, −20%, −25%, and −30% for gray and white matter blood flow values of 60 and 15, 80 and 20, 100 and 25, 120 and 30, and 140 and 35 m*l*/100 m*l*/min, respectively.

The simulated effects of gray-white matter mixing on the vascular response in CBF calculated by the ARG method are shown in Figure 4; the baseline blood flow values in gray and white matter are assumed to be 80 and 20 m*l*/100 m*l*/min, respectively. Because of tissue heterogeneity, the vascular response was systematically underestimated when CBF was greater than baseline CBF and overestimated when it was less than baseline CBF. Minimum vascular responses were 17%, 31%, and 43% when vascular responses in ideal CBF were +25%, +50%, and +75%, respectively. The maximum response was −21% when vascular responses in ideal CBF were −25%.

Images of ideal CBF, ARG-CBF, and the percentage of error in ARG-CBF in comparison to ideal CBF in the simulation study are shown in Figure 5. The values of ideal CBF, ARG-CBF, and percentage error of ARG-CBF for each ROI are also given in Table 4. ARG-CBF was systematically underestimated because of gray-white matter mixing. ARG-CBF in the neocortical regions was underestimated by −18% to −12%, −21% to −16%, −26% to −20%, −31% to −24%, and −35% to −27% for gray and white matter blood flow of 60 and 15, 80 and 20, 100 and

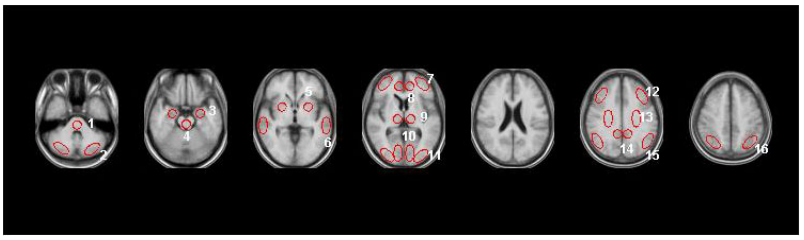

Fig. 1 Regions-of-interest drawn on all anatomically standardized images (1: pons, 2: cerebellar cortex, 3: parahippocampal gyrus, 4: midbrain, 5: putamen, 6: temporal cortex, 7: base of frontal cortex, 8: anterior cingulate gyrus, 9: thalamus, 10: cuneus of occipital cortex, 11: lateral side of occipital cortex, 12: convexity of frontal cortex, 13: centrum semiovale, 14: posterior cingulate gyrus, 15: inferior parietal cortex, 16: superior parietal cortex). All images are transaxial sections parallel to the anterior-posterior commissure (AC-PC) line. The slice positions are −36, −18, 0, 6, 22, 36, and 50 mm from the AC-PC line.

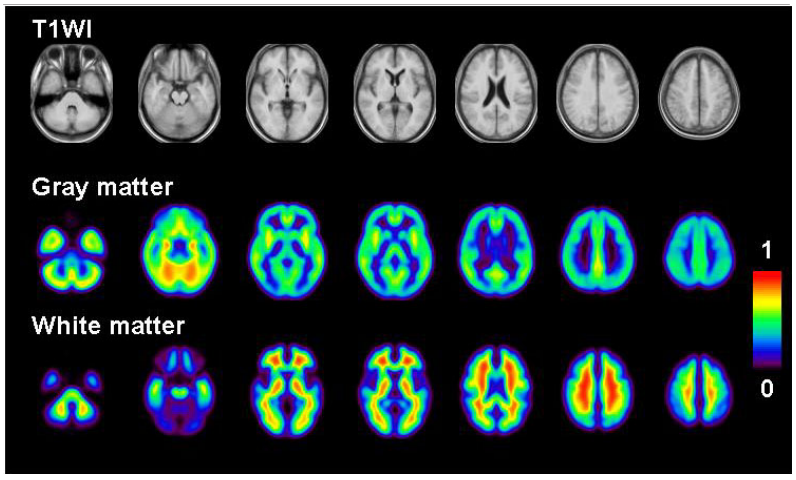

Fig. 2 Anatomically standardized averaged T1-weighted MR images and gray and white matter images. Scale maximum and minimum values are 1 and 0 m*l*/m*l*, respectively, for both gray and white matter images.

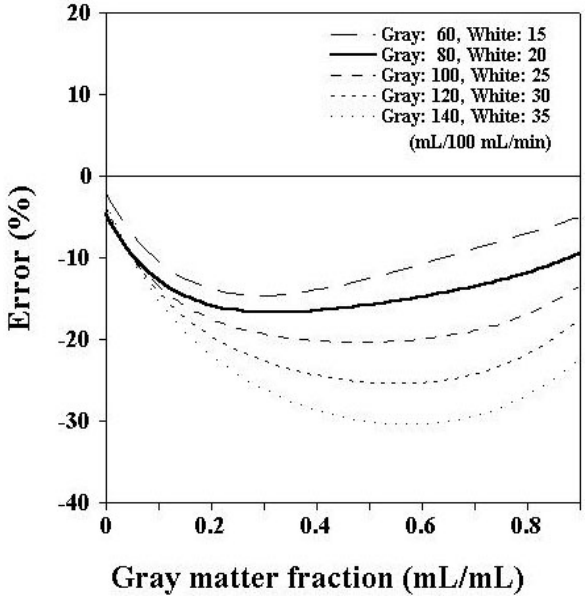

Fig. 3 Effects of gray-white matter mixing on CBF calculated by the ARG method. X-axis is the fraction of gray matter. The fraction of cerebrospinal fluid is assumed to be 0.1 m*l*/m*l*.

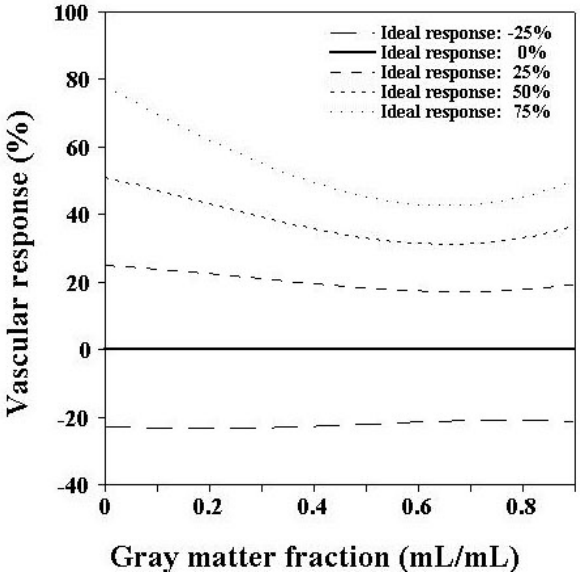

Fig. 4 Effects of gray-white matter mixing on vascular response in CBF calculated by the ARG method. Baseline blood flow values in gray and white matter are assumed to be 80 and 20 m*l*/100 m*l*/min, respectively. X-axis is the fraction of gray matter. The fraction of cerebrospinal fluid is assumed to be 0.1 m*l*/m*l*.

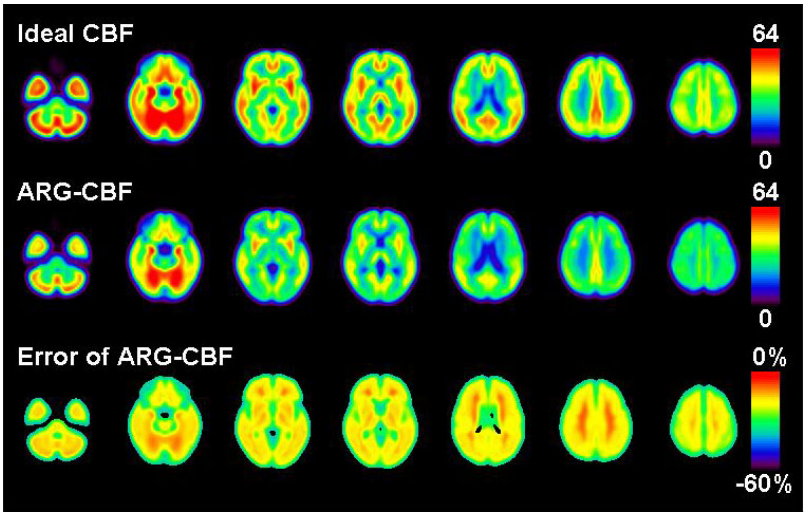

Fig. 5A

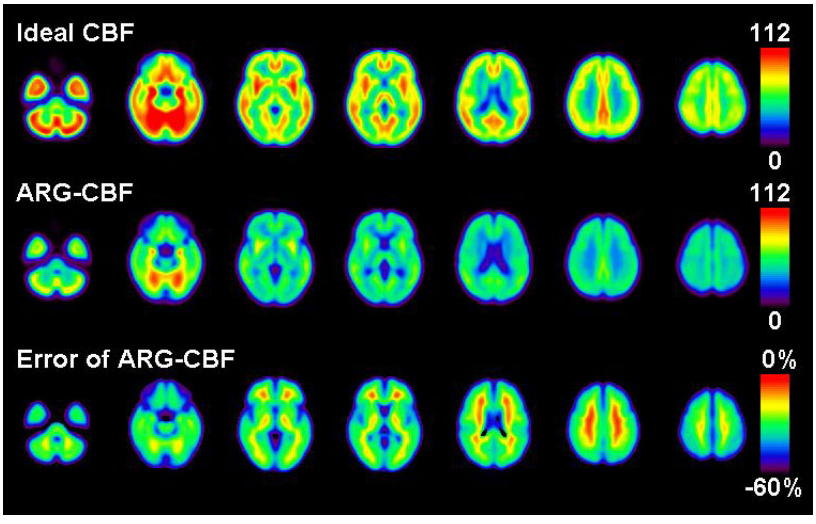

Fig. 5B

Fig. 5 Images of ideal CBF, ARG-CBF, and percentage of error in ARG-CBF in comparison to ideal CBF generated by simulation study. (A) Blood flow values in gray and white matter are assumed to be 80 and 20 m*l*/100 m*l*/min, respectively. Scale maximum and minimum values are 64 and 0 m*l*/100 m*l*/min, respectively, for images of ideal CBF and ARG-CBF. (B) Blood flow values in gray and white matter are assumed to be 140 and 35 m*l*/100 m*l*/min, respectively. Scale maximum and minimum values are 112 and 0 m*l*/100 m*l*/min, respectively, for images of ideal CBF and ARG-CBF.

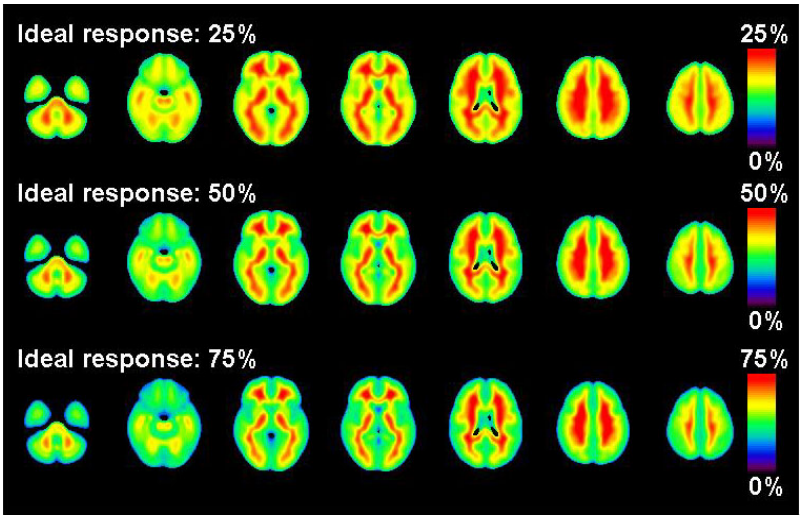

Fig. 6 Images of vascular response for ARG-CBF generated by simulation study. Baseline blood flow values in gray and white matter are assumed to be 80 and 20 m*l*/100 m*l*/min, respectively. Vascular responses in ideal CBF of 25%, 50%, and 75% correspond to gray and white matter blood flow values of 100 and 25, 120 and 30, and 140 and 35 m*l*/100 m*l*/min, respectively.

Table 4 Ideal CBF, ARG-CBF, and percentage error of ARG-CBF in comparison to ideal CBF in simulation study

Region	Ideal CBF (ml/100 ml/min)	ARG-CBF (ml/100 ml/min)	% error
Gray flow: 60, White flow: 15 (ml/100 ml/min)			
Cerebellum	43.5	39.7	−8.8
Pons	28.7	24.9	−13.6
Midbrain	30.4	26.1	−14.2
Thalamus	33.5	29.4	−12.2
Putamen	39.1	35.6	−9.1
Parahippocampal gyrus	47.0	43.2	−8.2
Anterior cingulate	34.9	30.5	−12.5
Posterior cingulate	36.1	32.1	−11.2
Frontal cortex base	31.7	27.0	−14.8
Frontal cortex convexity	32.8	27.9	−15.1
Temporal cortex	39.5	34.9	−11.9
Occipital cortex cuneus	34.6	30.2	−12.9
Lateral occipital cortex	29.0	24.9	−14.3
Inferior parietal cortex	34.2	29.7	−13.3
Superior parietal cortex	30.6	25.3	−17.6
Centrum semiovale	17.2	16.0	−6.5
Gray flow: 80, White flow: 20 (ml/100 ml/min)			
Cerebellum	58.0	50.5	−12.9
Pons	38.3	32.4	−15.6
Midbrain	40.6	33.8	−16.7
Thalamus	44.7	37.9	−15.0
Putamen	52.1	45.8	−12.2
Parahippocampal gyrus	62.6	54.7	−12.9
Anterior cingulate	46.6	39.1	−15.8
Posterior cingulate	48.2	41.2	−14.3
Frontal cortex base	42.2	34.7	−18.0
Frontal cortex convexity	43.7	35.7	−18.4
Temporal cortex	52.7	44.4	−16.0
Occipital cortex cuneus	46.2	38.8	−16.1
Lateral occipital cortex	38.6	32.2	−16.7
Inferior parietal cortex	45.7	38.2	−16.4
Superior parietal cortex	40.9	32.2	−21.3
Centrum semiovale	22.9	21.2	−7.6
Gray flow: 100, White flow: 25 (ml/100 ml/min)			
Cerebellum	72.5	59.6	−17.9
Pons	47.9	39.1	−18.5
Midbrain	50.7	40.4	−20.2
Thalamus	55.9	45.1	−18.8
Putamen	65.2	54.5	−16.4
Parahippocampal gyrus	78.3	64.3	−18.0
Anterior cingulate	58.2	46.3	−20.0
Posterior cingulate	60.2	48.8	−18.5
Frontal cortex base	52.8	41.2	−22.0
Frontal cortex convexity	54.6	42.3	−22.8
Temporal cortex	65.9	52.1	−21.2
Occipital cortex cuneus	57.7	45.9	−20.3
Lateral occipital cortex	48.3	38.7	−19.8
Inferior parietal cortex	57.1	45.2	−20.7
Superior parietal cortex	51.1	38.0	−25.7
Centrum semiovale	28.6	26.6	−7.1
Gray flow: 120, White flow: 30 (ml/100 ml/min)			
Cerebellum	86.9	67.2	−22.7
Pons	57.4	44.9	−21.9
Midbrain	60.9	46.1	−24.2
Thalamus	67.0	51.1	−22.9
Putamen	78.2	62.0	−20.6
Parahippocampal gyrus	93.9	72.5	−23.0
Anterior cingulate	69.8	52.1	−24.6
Posterior cingulate	72.2	55.2	−22.8
Frontal cortex base	63.3	46.5	−26.4
Frontal cortex convexity	65.5	47.6	−27.5
Temporal cortex	79.1	58.3	−26.5
Occipital cortex cuneus	69.2	51.8	−24.9
Lateral occipital cortex	57.9	44.3	−23.5
Inferior parietal cortex	68.4	51.0	−25.4
Superior parietal cortex	61.3	42.6	−30.5
Centrum semiovale	34.3	32.1	−6.4
Gray flow: 140, White flow: 35 (ml/100 ml/min)			
Cerebellum	101.4	73.7	−27.4
Pons	67.0	49.9	−25.5
Midbrain	71.0	50.8	−28.3
Thalamus	78.2	56.2	−27.1
Putamen	91.2	68.6	−24.6
Parahippocampal gyrus	109.6	79.0	−28.1
Anterior cingulate	81.5	57.0	−29.1
Posterior cingulate	84.3	60.5	−27.2
Frontal cortex base	73.9	50.9	−30.9
Frontal cortex convexity	76.4	51.9	−32.3
Temporal cortex	92.2	63.3	−31.6
Occipital cortex cuneus	80.8	56.7	−29.5
Lateral occipital cortex	67.6	49.1	−27.3
Inferior parietal cortex	79.9	55.8	−30.1
Superior parietal cortex	71.5	46.2	−35.4
Centrum semiovale	40.1	37.4	−6.4

25, 120 and 30, and 140 and 35 ml/100 ml/min, respectively.

Images of vascular response for ARG-CBF in the simulation study are shown in Figure 6; baseline blood flow values in gray and white matter are assumed to be 80 and 20 ml/100 ml/min, respectively. The vascular response values for ARG-CBF for each ROI are also given in Table 5. Because of gray-white matter mixing, the vascular response was systematically underestimated when CBF was greater than baseline CBF and overestimated when CBF was less than baseline CBF. The vascular responses in the neocortical regions ranged from −23% to −21%, from 17% to 20%, from 31% to 37%, and from 42% to 52% when vascular responses in ideal CBF were −25%, 25%, 50%, and 75%, respectively.

The vascular response values from ideal CBF values processed by Eqs. 2 and 3 with patient data obtained on the normal side and in the pons and midbrain are given in Table 6. After correction for effects of tissue heterogeneity, values of vascular response to acetazolamide stress ranged from 64% to 116% in the neocortical regions.

Table 5 Vascular response for ARG-CBF in simulation study. Baseline blood flow of gray and white matter are assumed to be 80 and 20 ml/100 ml/min, respectively

Region	Vascular response (%)			
	Gray flow (ml/100 ml/min):	60	100	120	140
	White flow (ml/100 ml/min):	15	25	30	35
	(Ideal response)	(−25%)	(25%)	(50%)	(75%)
Cerebellum		−21.4	17.8	33.0	45.8
Pons		−23.2	20.7	38.7	54.3
Midbrain		−22.7	19.7	36.4	50.5
Thalamus		−22.5	19.3	35.7	49.7
Putamen		−22.4	19.0	35.7	50.2
Parahippocampal gyrus		−21.0	17.5	32.3	44.2
Anterior cingulate		−22.1	18.6	34.0	46.8
Posterior cingulate		−22.2	18.9	34.9	48.4
Frontal cortex base		−22.0	18.7	34.1	46.9
Frontal cortex convexity		−21.9	18.2	33.0	45.0
Temporal cortex		−21.3	17.1	31.0	42.2
Occipital cortex cuneus		−22.2	18.6	34.0	46.8
Lateral occipital cortex		−22.8	20.1	37.4	52.2
Inferior parietal cortex		−22.2	18.5	33.7	46.2
Superior parietal cortex		−21.4	17.8	32.2	43.5
Centrum semiovale		−24.2	25.6	51.6	77.0

Table 6 Vascular response from ARG-CBF and from calculated ideal CBF in measured SPECT data

Region	Vascular response (%)	
	ARG-CBF	Ideal CBF
Cerebellum	44.5 ± 22.4	54.8 ± 29.5
Pons	44.2 ± 20.7	61.9 ± 44.9
Midbrain	42.0 ± 10.2	49.3 ± 18.7
Thalamus	40.6 ± 15.4	47.1 ± 27.1
Putamen	51.8 ± 18.6	60.0 ± 27.0
Parahippocampal gyrus	48.6 ± 18.0	48.6 ± 19.8
Anterior cingulate	47.4 ± 18.4	54.8 ± 27.8
Posterior cingulate	49.0 ± 23.2	53.9 ± 28.2
Frontal cortex base	51.5 ± 17.9	92.8 ± 51.0
Frontal cortex convexity	50.2 ± 16.9	71.7 ± 31.2
Temporal cortex	49.6 ± 17.8	64.4 ± 29.7
Occipital cortex cuneus	47.9 ± 18.5	116.3 ± 51.4
Lateral occipital cortex	48.8 ± 17.2	81.3 ± 38.7
Inferior parietal cortex	48.8 ± 22.2	72.8 ± 38.4
Superior parietal cortex	50.1 ± 16.1	113.3 ± 57.2
Centrum semiovale	44.4 ± 13.6	44.7 ± 13.9

Values are shown as mean ± SD.

DISCUSSION

Vascular responses to acetazolamide stress on the side contralateral to the brain region containing a lesion, which can be considered as approximately normal values of vascular response, ranged from 48% to 52% in the neocortical regions (Table 2). These values were in good agreement with previously reported normal vascular responses to acetazolamide stress measured by the ARG method.[11] Simulation studies show systematic underestimation of ARG-CBF due to the tissue heterogeneity, and systematic underestimation of vascular response in ARG-CBF when CBF is increased (Figs. 3, 4). These findings indicate that vascular responses to acetazolamide stress determined by the ARG method are systematically underestimated.

VBM analysis can be used to generate gray and white matter images from a T1-weighted MR image (Fig. 2, Table 3). Regional differences in the errors in CBF calculations by the ARG method due to tissue heterogeneity were simulated with the use of averaged gray and white matter images (Fig. 5, Table 4). In all brain regions, systematic underestimation of ARG-CBF was observed. The greatest degree of underestimation of ARG-CBF was observed in the superior parietal cortex and the smallest in the centrum semiovale. The degree of underestimation of ARG-CBF was smaller in the cerebellum, putamen, and parahippocampal gyrus than in the neocortical regions. These findings indicate that the error in ARG-CBF due to tissue heterogeneity is decreased in the more homogeneous tissue, i.e., tissue mainly containing gray matter or white matter.[12] It is noteworthy that the greatest degree of underestimation of ARG-CBF was observed in the superior parietal cortex, which often shows hypoperfusion in patients with Alzheimer disease.[26,27] This should be considered in the diagnosis of Alzheimer disease based on CBF images generated by the ARG method. The degree of underestimation of ARG-CBF due to tissue heterogeneity increased when CBF increased, indicating that tissue heterogeneity could affect the vascular response to acetazolamide stress.

Regional differences in the vascular response in ARG-CBF due to tissue heterogeneity were simulated with the use of averaged gray and white matter images (Fig. 6, Table 5). In all brain regions except the centrum semiovale, systematic underestimation of the vascular response was observed when CBF was increased in comparison to baseline CBF. In particular, the greatest underestimation of vascular response was observed in the temporal cortex and superior parietal cortex. Such regional differences should be considered in the estimation of cerebral vascular reserve.

Although the SPECT data were obtained from patients, not normal healthy subjects, we attempted to correct for the effects of tissue heterogeneity in the SPECT data. A limitation of this correction is that tissue fractions of gray and white matter might be different between patients and healthy subjects. After correction for these effects, values of the vascular response to acetazolamide stress ranged from 64% to 116% in the neocortical regions (Table 6). These values were 30–140% greater than values from CBF calculated by the ARG method. Such a discrepancy in the vascular responses to acetazolamide stress between the CBF values determined by the ARG method and CBF values corrected for the effects of tissue heterogeneity should be considered in the estimation of cerebral vascu-

lar reserve. However, assessment of the vascular response to acetazolamide stress is more important at the lower range of response, i.e., 0% to 20% vascular response, for treatment planning and prediction of outcome in patients with major cerebral arterial occlusive disease.[6,7] In this low range of vascular response, the effect of tissue heterogeneity may not be significant.

In the present estimation of the effect of tissue heterogeneity, all images were smoothed with an isotropic Gaussian kernel at a FWHM of 10 mm, which matched the FWHM of the SPECT scanner. When the spatial resolution of the SPECT scanner is changed, the effect of tissue heterogeneity may be changed. Further investigation is necessary to estimate the effect of spatial resolution on tissue heterogeneity effects.

In conclusion, we estimated errors in CBF and the vascular response to acetazolamide stress determined by the ARG method which were due to a mixture of gray and white matter, using images of gray and white matter fraction derived from MR images by VBM analysis. Systematic underestimation of CBF was observed in all brain regions. The vascular response was also systematically underestimated in almost all brain regions. Such underestimation of the vascular response to acetazolamide stress due to tissue heterogeneity should be considered in the estimation of cerebral vascular reserve.

ACKNOWLEDGMENTS

This work was supported by a Grant-in-Aid for Scientific Research (C) (No. 15591314) from the Japan Society for the Promotion of Science, a 21st Century COE Program Special Research Grant for "Future Medical Engineering Based on Bionanotechnology", and Health and Labour Science Research Grants for Research on Advanced Medical Technology (H14-Nano-020). The assistance of members of the Tohoku University Hospital staff in performing the SPECT experiments is also gratefully acknowledged.

REFERENCES

1. Winchell HS, Baldwin RM, Lin TH. Development of I-123-labeled amines for brain studies: localization of I-123 iodophenylalkyl amines in rat brain. *J Nucl Med* 1980; 21: 940–946.
2. Winchell HS, Horst WD, Braun L, Oldendorf WH, Hattner R, Parker H. *N*-isopropyl-[^{123}I] *p*-iodoamphetamine: single-pass brain uptake and washout; binding to brain synaptosomes; and localization in dog and monkey brain. *J Nucl Med* 1980; 21: 947–952.
3. Raynaud C, Rancurel G, Samson Y, Baron JC, Soucy JP, Kieffer E, et al. Pathophysiologic study of chronic infarcts with I-123 isopropyl iodo-amphetamine (IMP): the importance of periinfarct area. *Stroke* 1987; 18: 21–29.
4. Ito H, Iida H, Bloomfield PM, Murakami M, Inugami A, Kanno I, et al. Rapid calculation of regional cerebral blood flow and distribution volume using iodine-123-iodoamphetamine and dynamic SPECT. *J Nucl Med* 1995; 36: 531–536.
5. Powers WJ, Grubb RL, Raichle ME. Physiological responses to focal cerebral ischemia in humans. *Ann Neurol* 1984; 16: 546–552.
6. Kuroda S, Houkin K, Kamiyama H, Mitsumori K, Iwasaki Y, Abe H. Long-term prognosis of medically treated patients with internal carotid or middle cerebral artery occlusion: can acetazolamide test predict it? *Stroke* 2001; 32: 2110–2116.
7. Ogasawara K, Ogawa A, Yoshimoto T. Cerebrovascular reactivity to acetazolamide and outcome in patients with symptomatic internal carotid or middle cerebral artery occlusion: a xenon-133 single-photon emission computed tomography study. *Stroke* 2002; 33: 1857–1862.
8. Iida H, Itoh H, Nakazawa M, Hatazawa J, Nishimura H, Onishi Y, et al. Quantitative mapping of regional cerebral blood flow using iodine-123-IMP and SPECT. *J Nucl Med* 1994; 35: 2019–2030.
9. Ito H, Ishii K, Atsumi H, Inukai Y, Abe S, Sato M, et al. Error analysis of autoradiography method for measurement of cerebral blood flow by ^{123}I-IMP brain SPECT: a comparison study with table look-up method and microsphere model method. *Ann Nucl Med* 1995; 9: 185–190.
10. Iida H, Akutsu T, Endo K, Fukuda H, Inoue T, Ito H, et al. A multicenter validation of regional cerebral blood flow quantitation using [^{123}I]iodoamphetamine and single photon emission computed tomography. *J Cereb Blood Flow Metab* 1996; 16: 781–793.
11. Ogasawara K, Ito H, Sasoh M, Okuguchi T, Kobayashi M, Yukawa H, et al. Quantitative measurement of regional cerebrovascular reactivity to acetazolamide using ^{123}I-*N*-isopropyl-*p*-iodoamphetamine autoradiography with SPECT: validation study using $H_2{}^{15}O$ with PET. *J Nucl Med* 2003; 44: 520–525.
12. Herscovitch P, Raichle ME. Effect of tissue heterogeneity on the measurement of cerebral blood flow with the equilibrium $C^{15}O_2$ inhalation technique. *J Cereb Blood Flow Metab* 1983; 3: 407–415.
13. Iida H, Kanno I, Miura S, Murakami M, Takahashi K, Uemura K. A determination of the regional brain/blood partition coefficient of water using dynamic positron emission tomography. *J Cereb Blood Flow Metab* 1989; 9: 874–885.
14. Ashburner J, Friston KJ. Voxel-based morphometry—the methods. *Neuroimage* 2000; 11: 805–821.
15. Kimura K, Hashikawa K, Etani H, Uehara A, Kozuka T, Moriwaki H, et al. A new apparatus for brain imaging: four-head rotating gamma camera single-photon emission computed tomograph. *J Nucl Med* 1990; 31: 603–609.
16. Chang LT. A method for attenuation correction in radionuclide computed tomography. *IEEE Trans Nucl Sci* 1978; 25: 638–643.
17. Chang LT. Attenuation correction and incomplete projection in single photon emission computed tomography. *IEEE Trans Nucl Sci* 1979; 26: 2780–2789.
18. Friston KJ, Frith CD, Liddle PF, Dolan RJ, Lammertsma AA, Frackowiak RS. The relationship between global and local changes in PET scans. *J Cereb Blood Flow Metab* 1990; 10: 458–466.
19. Inoue K, Ito H, Nakagawa M, Goto R, Yamazaki T, Fukuda H. Regional differences in distribution volume of I-123

IMP in the human brain: effect on CBF calculated by ARG method. *Ann Nucl Med* 2002; 16: 311–316.
20. Ito H, Inoue K, Goto R, Kinomura S, Sato T, Kaneta T, et al. Error analysis of measured cerebral vascular response to acetazolamide stress by I-123-IMP autoradiographic method with single photon emission computed tomography: errors due to distribution volume of I-123-IMP. *Ann Nucl Med* 2004; 18: 221–226.
21. Iida H, Itoh H, Bloomfield PM, Munaka M, Higano S, Murakami M, et al. A method to quantitate cerebral blood flow using a rotating gamma camera and iodine-123 iodoamphetamine with one blood sampling. *Eur J Nucl Med* 1994; 21: 1072–1084.
22. Hoedt-Rasmussen K. Regional cerebral flow in man measured externally following intra-arterial administration of ^{85}Kr or ^{133}Xe dissolved in saline. *Acta Neurol Scand Suppl* 1965; 14: 65–68.
23. Iida H, Law I, Pakkenberg B, Krarup-Hansen A, Eberl S, Holm S, et al. Quantitation of regional cerebral blood flow corrected for partial volume effect using O-15 water and PET: I. theory, error analysis, and stereologic comparison. *J Cereb Blood Flow Metab* 2000; 20: 1237–1251.
24. Bereczki D, Wei L, Otsuka T, Hans FJ, Acuff V, Patlak C, et al. Hypercapnia slightly raises blood volume and sizably elevates flow velocity in brain microvessels. *Am J Physiol* 1993; 264: H1360–1369.
25. Ito H, Yokoyama I, Iida H, Kinoshita T, Hatazawa J, Shimosegawa E, et al. Regional differences in cerebral vascular response to P_aCO_2 changes in humans measured by positron emission tomography. *J Cereb Blood Flow Metab* 2000; 20: 1264–1270.
26. Kogure D, Matsuda H, Ohnishi T, Asada T, Uno M, Kunihiro T, et al. Longitudinal evaluation of early Alzheimer's disease using brain perfusion SPECT. *J Nucl Med* 2000; 41: 1155–1162.
27. Petrella JR, Coleman RE, Doraiswamy PM. Neuroimaging and early diagnosis of Alzheimer disease: a look to the future. *Radiology* 2003; 226: 315–336.